J. Phys. Chem. A **2008,** *112,* 989−999

Effect of a Water Molecule on the Sugar Puckering of Uridine, 2′-Deoxyuridine, and 2′-*O*-Methyl Uridine Inserted in Duplexes

Sophie Barbe[†] **and Marc Le Bret***

LBPA, CNRS, Ecole Normale Supérieure de Cachan, 61 Avenue du Président Wilson, 94235 Cachan, France

Received: July 23, 2007; In Final Form: November 2, 2007

We used high-level quantum mechanical calculations to determine the pucker (north type or south type) of various compounds: uridine, 2′-deoxyuridine, and 2′-O-methyl uridine. Although the dihedrals of the backbone are set close to their experimental values in double-stranded nucleic acids, calculations using density functional theory show that, in vacuo or in a continuum mimicking the dielectric properties of water, the south puckering conformations of uridine is favored. This contrasts with experimental data: most ribonucleosides inserted into a duplex have the north puckering. We show here that the north puckering is favored when an explicit water molecule is introduced into the calculation. The orientations of the 2′ group and of the water molecule have implications for the prevalence of the north puckering. We studied several orientations of the water molecule binding uracil O_2 and the 2′ group and estimated the energy barriers in the path between the north-to-south conformations. The north puckering is more favored in 2′-OH than in 2′-OCH_3 compounds in the presence of the explicit water molecule.

Introduction

RNA contains ribose whereas DNA contains 2′-deoxyribose. The presence of the 2′-hydroxyl group on the RNA furanose sugar ring is the reason for the major structural and dynamic differences between RNA and DNA molecules; it is sufficient to confine RNA double helices almost exclusively to a single structural family (the A form), whereas DNA is polymorphic and exists in a variety of structural families including the A, B, and Z forms.[1]

Structural and biophysical studies indicate that the additional hydroxyl group stabilizes the C3′-endo or north (N) sugar pucker (Figure 1) in RNA duplexes, whereas the C2′-endo or south (S) sugar pucker is only prevalent in double-stranded DNA systems.[1−4] The RNA duplexes are considered as rigid since they are found almost exclusively in the N conformation,[5,6] whereas the distribution of the puckering in double stranded DNAs is relatively broad.[6,7] Indeed, this 2′-hydroxyl group has major structural implications because it is involved in recognition, processing, and catalytic properties of RNA,[8−10] including the transesterification reactions involved in the group I and group II splicing reactions,[8−10] self-cleavage in lariat-RNA,[9] and RNA catalysis in ribozyme and in ribonuclease activities.[8] An understanding of the orientations and the dynamics of the 2′-hydroxyl bond is essential for elucidating its specific structural consequences concerning the stabilization of helical regions, complex RNA tertiary folds, and RNA/protein interactions. This knowledge is also important for studying the mechanisms of catalytic RNA molecules. Crystallographic studies,[11] NMR analyses,[12,13] and dynamic simulations[14] suggest various possible orientations of this 2′-OH.

Because of the role played by the hydroxyl substitution at 2′, ribose containing other 2′ substitutions have been investigated. Modified oligonucleotides are important for many applications, including antisense therapeutics, diagnostics, profiling gene expression with microarrays, identifying bands on gels by Northern blotting and probing RNA structure. Oligonucleotides with 2′-O-methyl modifications can be particularly useful for various applications because they are easily synthesized and chemically stable, and they form duplexes that have a melting temperature higher than that of their unmodified counterparts.[15,16] There is probably an additional sequence effect as the melting temperature of a DNA duplex containing only one 2′-O-methyl modification was found lower than in the natural fragment.[17] The 2′-O-methyl nucleosides in duplexes are found in the N conformation.[18−22] The methyl group attached to the $O_{2'}$ atom points toward the minor groove.[18−22]

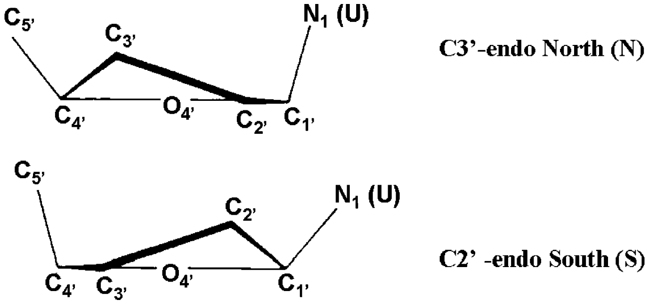

Figure 1. Sugar puckering definition. Because of the valence angles, the energetically most favored conformation of the five-membered cycle $C_{1'}$, $C_{2'}$, $C_{3'}$, $C_{4'}$, and $O_{4'}$ is not planar. Usually, either $C_{2'}$ or $C_{3'}$ is off the average plane defined by the other atoms. $C_{2'}$ is endo when it lies on the same side as $C_{5'}$. In that case, the sugar puckering is called south (S). $C_{3'}$ is endo when it lies on the same side as $C_{5'}$. In that case, the sugar puckering is called north (N).

Although less efficient than the addition of a group at 2′, solvent interactions are a key factor in the conformational variability[23−25] and ligand binding[26−32] of nucleic acids. The N puckering of desoxynucleotides is more frequently observed in less hydrated media[1,6,33−35] or in DNA−protein complexes.[6,36]

Given the presence of such a variety of experimental data, the task of theoretical investigations is challenging. The first

---

* Corresponding author. Phone: +33 147405997. Fax: +33 147407659. E-mail: mlebret@lbpa.ens-cachan.fr.

[†] E-mail: sbarbe@insa-toulouse.fr.

10.1021/jp075777u CCC: $40.75

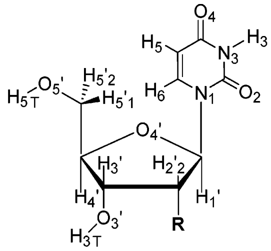

Compounds	R
H-U	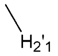
OH-RIB-U	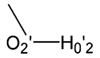
OCH3-RIB-U	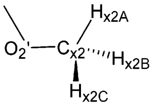

Figure 2. Atom numbering and chemical structure of the compounds studied.

attempts to predict to sugar puckering were empirical rules derived from studies on mononucleosides. Gauche effects,[37−42] anomeric effects,[38,40,41,43−46] and electronegativity[47,48] assessed from a set of experimental structures have been used to predict the conformation of a modified or natural nucleoside. However, whether alone or incorporated in double-stranded fragments, nucleosides or nucleotides have a different distribution of puckering. Monoribonucleotides, free in solution, have a significant population of S conformers.[43]

The quantum mechanical approach is however more reliable in two ways: (i) it implicitly takes into account the various effects and (ii) the study can be restricted to the conformations having dihedrals analogous to their values in a double helix. If hydrogen bonds that cannot exist in duplexes are allowed, ab initio calculations on ribonucleosides[49] show that the energy gap between the N and the S conformations is very small. If they are hindered by carefully orienting the distal hydrogen atoms, natural deoxynucleosides are mainly found in the S conformation, but the minor N population is correctly predicted.[50,51] Compounds with a 2′-OH furanose are found prevalently in the N conformation[7,52] when only the conformations compatible with double helical conformations are considered.

We report a conformational study of three compounds which differ by the 2′ substituent: uridine, 2′-deoxyuridine, and 2′-O-methyl uridine. Hydration is important, so we report calculations in vacuo, in a continuous medium mimicking the dielectric properties of water, and in the presence of an explicit water molecule. The aim was to determine the contributions of the 2′ substituent and of the hydration to the conformation of natural and 2′-modified nucleosides inserted in duplexes and to develop a model that satisfactorily describes the furanose puckering.

Methods

Gaussian 03 programs[53] with the 6-31G(d) basis set were used for quantum mechanical calculations. Energy minimizations were performed to the default tolerances in the Gaussian programs. All degrees of freedom, other than those specified as being fixed, including all bond lengths and angles, were allowed to relax during the energy minimizations.

All structures were minimized using the density functional theory/Becke 3, Lee, Yang, and Par (DFT/B3LYP) level which considers explicitly the correlation effects. The energy of the conformation was then estimated using the largest basis that could be used on our computer: 6-311++G(3df,2pd) and 6-311++G(2df,2pd) respectively for 2′-OH and 2′-OCH3 compounds. As DFT methods do not fully evaluate the dispersion forces, MP2 (second-order Møller-Plesset correction) calculations were also performed with the basis 6-31G(d). However, MP2/6-311+G(2d,p) failed.

The effect of the solvent was estimated in two different ways: (i) the conductor-like polarizable continuum model (CPCM) method[54,55] was used to embed the nucleoside in a continuous medium with the dielectric properties of water; and (ii) a water molecule was added to the nucleoside, and the complex was minimized in vacuo. In H−U (Figure 2), the water molecule was initially positioned with one of its protons, H_{2WT}, in contact with the O_2 atom of the uracil as suggested by data bank analysis.[6,56] In OH-RIB-U (Figure 2), the water molecule was initially positioned to form a bridge between the O_2 of the uracil and the 2′-group, as described in Figure 4 of Egli et al. paper.[11] The water molecule in OCH3-RIB-U has been set close to O_2 as it is in the 2′-OMe(CGCGCG)$_2$ duplex.[19,22]

The dihedral angles in the nucleosides (Figure 2) are defined as follows:

$$\beta \qquad \gamma \qquad \delta \qquad \varepsilon$$

$$H_{5T} - O_{5}' - C_{5'} - C_{4'} - C_{3'} - O_{3'} - H_{3T}$$

The glycosidic angle χ, is defined as $O_{4'}-C_{1'}-N_9-C_4$ for purines and $O_{4'}-C_{1'}-N_1-C_2$ for pyrimidines. The five endocyclic dihedral angles were approximated by a Fourier analysis giving the phase or pseudorotation angle (P) and the amplitude (τ) according to Rao et al.:[57]

$$\tau_j = \tau \cos[P + 4\pi(j - 2)/5] \qquad (1)$$

A and B are computed from the measurements of the dihedrals τ_j in a conformation:

$$A = 2/5 \sum_{j=0}^{4} \tau_j \cos[4\pi(j - 2)/5] \qquad (2)$$

$$B = -2/5 \sum_{j=0}^{4} \tau_j \sin[4\pi(j - 2)/5] \qquad (3)$$

The amplitude, τ, and the pseudorotation, P, are given by:

$$\tau = (A^2 + B^2)^{1/2} \qquad (4)$$

$$P = \tan^{-1} B/A \qquad (5)$$

The pseudorotation space is divided into four equally sized quadrants centered around $P = 0.0°$, $P = 90.0°$, $P = 180.0°$, and $P = -90.0°$ that are referred to as the north (N), east (E), south (S), and west (W) quadrants, respectively.

When locating the north and south energy minima, the initial furanose conformations were set in canonical N and S puckering, respectively. In these calculations, the dihedral angles β, γ, and χ were assigned to modal values obtained from the crystal nucleic acid structure database[6] as follows:

$$\beta = 175° \pm 15, \quad \gamma = 57° \pm 10 \quad \text{and} \quad \chi = -161° \pm 11 \ (\text{anti}^{(-\text{ap})}) \quad \text{for N-type conformations;}$$

$$\beta = 168° \pm 25, \quad \gamma = 51° \pm 16 \quad \text{and} \quad \chi = -108° \pm 11 \ (\text{anti}^{(-\text{ac})}) \quad \text{for S-type conformations.}$$

The ϵ energy profile of a furanose substituted in 3′ by a $O_{3'}$-phosphate group shows three minima with both S and N puckering.[50] Two minima, in −ap and −sc are much more favorable than the third. Therefore, in addition to the puckering and the dihedrals β, γ, and χ, the dihedral ϵ was set in −ap or −sc before optimization. In most cases, the dihedrals are unconstrained during the minimization. When the furanose of the minimized conformation is S-type with ϵ in −ap or −sc, the conformation would be called B_I or B_{II} if the model contained a phosphate group at the 5′ end. To underline the fact that, here, there is no ζ, the conformations are called B_I-like or B_{II}-like forms. Similarly, when the furanose is in the N conformation, the minima, with ϵ in −ap and −sc, are called A-like and A_{II}-like forms, respectively. For OH-RIB-U and OCH3-RIB-U compounds, some A-like and B_I-like conformations were minimized by constraining the ϵ dihedral angle at −155.0° to avoid the formation of the $H_{3T}\cdots O_{2'}$ hydrogen bond which cannot exist in polynucleotide chains.

For OH-RIB-U, calculations were performed starting from two different starting models with different dihedral λ: ($C_{3'}-C_{2'}-O_{2'}-H_{O'2}$). In model 1, the 2′-group points away from the $O_{3'}$ atom. In model 2, the 2′-group points to the $O_{3'}$ atom. In some cases, λ had to be constrained, during a preliminary minimization. For OCH3-RIB-U, λ ($C_{3'}-C_{2'}-O_{2'}-C_{X2}$) was set to rotate the methyl group away from $O_{3'}$. Conformations were manipulated and analyzed using our program MORCAD.[58]

Potential energy differences were calculated to investigate the relation of conformation to energetics in the compounds studied. The energy of the B_I-like conformation was taken as the reference ($\Delta E = 0$). The east energy barrier, Be, separating the A-like and B_I-like conformations, is approximated by the energy of the $O_{4'}$ endo conformation of the furanose (endocyclic dihedral angle τ_2 ($C_{1'}-C_{2'}-C_{3'}-C_{4'}$) = 0.0°) relative to either A-like or B_I-like conformations, whichever is the more stable, consistent with other similar studies.[50]

In this work, the hydrogen bonds are defined as follows: a D−H donor group and an electronegative acceptor atom A form a hydrogen bond when the distance D−H is less than 2.7 Å and the angle D−H−A is greater than 90°.

Results and Discussion

H−U. With each method of calculations, four unconstrained minima are obtained for the deoxyribonucleoside H−U (Figure 2): two with N puckering and two others with S puckering (Table 1). In each conformation, the values of dihedral angles β, γ, δ (not shown here), ϵ, and χ (shown in Table 1) are close to their modal values. The four minimized conformations can easily be assimilated to analogues of A, A_{II}, B_I, and B_{II} forms.

In vacuo, the four minimized conformations appear in the order B_I-like < A-like < B_{II}-like < A_{II}-like (Table 1). As expected for a deoxyribonucleoside, the most favorable energetic conformation is B_I-like, and the most unfavorable is A_{II}-like. Analysis of the nucleic acid database[6] shows that the ratio B_I/B_{II} (populations in B_I and B_{II} conformations) is in the 2.41 to 2.64 range.[59] This ratio agrees remarkably well with our calculated energy gap: 0.6 kcal/mol (Table 1). The energy gap between A-like and B_I-likeconformations is half that determined at the MP2/6-31G(d) level of theory.[51]

In implicit solvent, the four minimized conformations appear in the order B_{II}-like < B_I-like < A-like < A_{II}-like (Table 1). This model predicts a much larger B_{II}-like population than is reported in the data banks. We therefore studied another model.

In DNA, according to X-ray databank analysis and molecular dynamics simulation, there is a hydration site near the pyrimidine O_2.[4,6,56] We therefore performed calculations in the presence of an explicit water molecule which was initially positioned with one of its protons, H_{2WT}, in contact with the O_2 atom of the uracil. In this case, the four minimized conformations appear in the order B_I-like < A-like < B_{II}-like < A_{II}-like (see Table 1). The energy classification of the four conformations is identical to that obtained in vacuo. However, the energy gap between the B_I-like and A-like conformations is approximately twofold that found in vacuo. This model predicts a B_I-like/B_{II}-like ratio around 5 which is slightly larger than the value obtained from the data banks.[59] The A_{II}-like conformation is in all situations the most unfavorable conformation, as expected.

Because of the absence of strong hydrogen bonds in the phosphodiester chain, weak hydrogen bonds, such as C−H⋯O and C−H⋯N, contribute to the conformational stability of nucleic acids.

Figure 3a shows the hydrogen bonds stabilizing the B_I-like and A-like conformations in vacuo. The S conformations are stabilized by the $C_{2'}-H_{2'}\cdots O_{5'}$ hydrogen bond. The N conformations are stabilized by a $C_{3'}-H_{3'}\cdots O_{5'}$ hydrogen bond. As experimentally observed[60,61] and well-simulated in silico,[62] the formation of the $C_6-H_6\cdots O_{5'}$ hydrogen bond stabilizes the antipyrimidine bases in nucleosides and nucleotides in the S and N conformations although the glycosidic angle χ differs by approximately 30°.[63] Both S and N conformations are further stabilized by the bonds $C_{1'}-H_{1'}\cdots O_2$ and $C_6-H_6\cdots O_{4'}$.

The S and N conformations obtained in the presence of an explicit water molecule in contact with O_2 are stabilized by the same hydrogen bonds observed in vacuo and in implicit solvent. However, supplementary hydrogen bonds between the nucleoside and the water molecule were also observed. The interaction $H_{2WT}\cdots O_2$ stabilizes both B_I-like and A-like conformations (Figure 3b). In the S conformations, H_{1WT} interacts with $O_{3'}$, but it remains free in the N conformations. Therefore, the orientation of the water molecule differs in the N and S conformations.

OH-RIB-U. The conformational analysis of the ribonucleoside OH-RIB-U is much more complicated than that of deoxyuridine, because of the simultaneous presence of the hydroxyl groups at 2′ and 3′. Because of these difficulties, the calculations that can be found in the literature have not shown that the N puckering is favored over the S as we now briefly review.

When a ribose alone[62] or a ribose attached to a pyrrole cycle[52] were minimized without constraints, the S conformation was found to be more favorable than the N conformation. Minimizations without constraints of the ribonucleosides rA, rU, and rG give two minima, N and S, of almost the same energy.[49] The N conformations are stabilized by an $O_{2'}-H_{O'2}\cdots O_{3'}$ hydrogen bond and the S conformations by an $O_{3'}-H_{3T}\cdots O_{2'}$ hydrogen bond.[49] Clearly, the latter is not found in RNA structures, except at the 3′ termini. A tempting solution is to study 3′-methyl phosphate-uridine instead of uridine. However, at the B3LYP/6-31G† level of theory,[62] the S conformation of 3′-methyl phosphate-uridine is more stable than its N conformation by 0.44 kcal/mol. To eliminate the hydrogen bond donor properties

TABLE 1: H−U Conformational Angles (Degrees) and Relative Energy Values, Δ*E* (Kilocalories per Mole)[a]

method of calculation	P	τ	ϵ	χ	ΔE	analogous form
B3LYP/6-31G(d)	14.30	35.8	−89.32	−158.61	0.98	A_{II}
	12.96	34.7	−169.54	−159.72	0.43	A
	167.75	34.8	−65.04	−126.33	0.60	B_{II}
	165.08	34.8	174.31	−130.14	0.00	B_I
B3LYP/CPCM/6-31G(d)	11.61	34.4	−89.04	−157.82	1.13	A_{II}
	11.80	34.9	−167.99	−156.50	1.12	A
	173.24	35.0	−66.06	−126.38	−0.03	B_{II}
	172.90	35.1	177.42	−127.47	0.00	B_I
B3LYP/6-31G(d) + WT	17.17	35.4	−86.82	−158.90	1.46	A_{II}
	16.17	33.9	−170.35	−159.62	1.00	A
	158.59	38.5	−58.54	−146.11	1.06	B_{II}
	158.87	38.4	−166.19	−139.08	0.00	B_I

[a] P, pseudorotation angle (see eq 5), τ, puckering amplitude (see eq 4), and dihedrals ϵ and χ are defined in Methods. Δ*E* is reported relative to the energy of the B_I-like conformation.

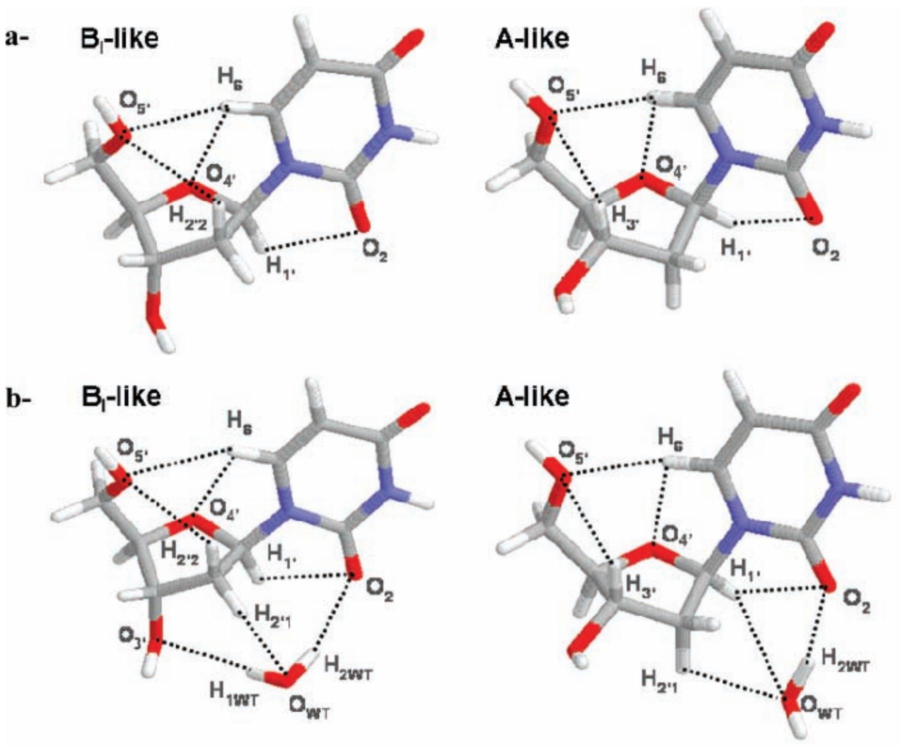

Figure 3. B_I-like and A-like conformations of H−U obtained by geometry optimization at the B3LYP/6-31G(d) level of theory (a). B_{II}-like and A-like conformations of H−U obtained by geometry optimization from the B3LYP/6-31G(d)+WT method of calculation (b). Hydrogen bonds are represented with dashed lines.

of the $O_{3'}-H_{3T}$ group and thus disfavor the S conformation, the dihedral ϵ was constrained to a value observed in RNA: as required, the pucker of a ribose attached to an imidazole ring[7] or a pyrrole cycle[52] was found in N. Therefore, here, OH-RIB-U was initially minimized freely. If the $O_{3'}-H_{3T}\cdots O_{2'}$ hydrogen bond formed, the minimization was restarted constraining the dihedral ϵ to −155°, a value consistent with both the A and the B_I forms.

Egli et al.[11] have shown that water molecules extensively hydrate the minor groove. Their high-resolution crystal structure of an RNA duplex shows that water molecules form clusters, positioned around the $O_{4'}$ and the $O_{2'}$ atoms. Water molecules near the hydroxyl group at 2′ are of particular significance because, in addition to their interactions with $O_{2'}$, they form secondary contacts that order the structure of the water in the minor groove. One of these water molecules forms an intraresidue bridge between $O_{2'}$ and pyrimidine O_2.

Simulation of the molecular dynamics of *t*RNA^{Asp} shows that $H_{O'2}$ in S-type and N-type riboses points preferentially toward the $O_{3'}$ oxygen of the same residue.[14] When the ribose is N-type, it can also point to pyrimidine O_2. NMR studies indicate that $H_{O'2}$ points away from the $O_{3'}$ of the same residue in RNA duplexes and DNA/RNA hybrids.[13] When a ribose attached to an imidazole group[7] is minimized at the MP2/6-31G(d) level, the N conformation is found to be more favorable than the S conformation ($\Delta E = -2.3$ kcal/mol) if $H_{O'2}$ points to the $O_{3'}$ atom in both conformations.

This led us to use a natural nucleoside to test whether the more stable conformation could be predicted from the orientation of $H_{O'2}$ by itself. We describe two models: in model 1, $H_{O'2}$ is set away from $O_{3'}$; in model 2, $H_{O'2}$ points to $O_{3'}$.

Model 1 ($H_{O'2}$ Set Away from $O_{3'}$). The $H_{O'2}$ proton of OH-RIB-U was set away from the $O_{3'}$ atom in the starting conformations. The ϵ dihedral angle was constrained in its modal values in the A-like and B_I-like conformations, but no other dihedral angle was forced during the minimizations. As for the study of H−U, the minimizations were performed in vacuo, B3LYP/6-31G(d), in implicit solvent, B3LYP/CPCM/6-31G(d), and in the presence of an explicit water molecule.

TABLE 2: Conformational Angles (Degrees) and Relative Energy Values (Kilocalories) of OH-RIB-U in Model 1 ($H_{O'2}$ Set Away from $O_{3'}$)[a]

method of calculation	P	τ	ϵ	χ	ΔE_1	analogous form
B3LYP/6-31G(d)	16.17	38.9	−92.96	−162.78	3.60	A_{II}
	17.07	35.5	−155.00[b]	−163.34	2.67	A
	−170.69	34.0	−75.33	−172.25	3.17	“B_{II}”
	−177.51	33.1	−155.00[b]	−171.71	0.00	“B_I”
B3LYP/CPCM/6-31G(d)	9.96	38.8	−92.77	−159.36	0.42	A_{II}
	10.40	37.7	−155.00[b]	−160.08	−0.02	A
	173.91	37.9	−67.33	−124.52	0.38	B_{II}
	172.41	36.7	−155.00[b]	−123.68	0.00	B_I
B3LYP/6-31G(d) + WT	13.30	41.2	−90.64	−159.01	−1.33	A_{II}
	12.41	39.2	−155.00[b]	−159.46	−2.06	A
	171.28	35.3	−74.45	−128.21	3.58	B_{II}
	167.81	33.6	−155.00[b]	−129.29	0.00	B_I

[a] ΔE_1 is reported relative to the energy of the model 1 B_I-like conformation. P, τ, ϵ, and χ are defined in the methods section. [b] Dihedral angle ϵ constrained during the minimization.

In vacuo, four minima are obtained: two of them are N-type and the other two are S-type (Table 2). In the N conformations, the values of dihedral angles β, γ, δ (not shown here), ϵ, and χ (Table 2) lie in the conformational ranges and can be called A-like and A_{II}-like forms. For the same reasons, the S conformations could be called B_I-like and B_{II}-like conformations, if the dihedral angle χ is −ac. As χ is in the −ap range, the S-type minima are called “B_I-like” and “B_{II}-like”. The four minimized conformations appear in the order “B_I-like” < A-like < “B_{II}-like” < A_{II}-like (see Table 2). The “B_I-like” conformation is very favorable, which does not agree with experimental data. In the “B_I-like” and “B_{II}-like” conformations, the anomalous glycosidic angles are favored because the $H_{O'2}$ hydrogen of the 2′-hydroxyl is strongly attracted by the O_2 atom of the uracil (Figure 4a). This interaction is so strong that it destroys the $C_6{-}H_6{\cdots}O_{5'}$ and $C_{1'}{-}H_{1'}{\cdots}O_2$ hydrogen bonds that are normally observed in the S conformations. The N conformations of OH-RIB-U are stabilized by the same four hydrogen bonds normally observed in the N conformations of H−U obtained both in vacuo and in implicit solvent. Minimizations in the presence of implicit water with the CPCM method were performed to dampen the effect of the $O_{2'}{-}H_{O'2}{\cdots}O_2$ hydrogen bond. This generated four minima corresponding to the A-like, A_{II}-like, B_I-like, and B_{II}-like conformations. These four minimized conformations appear in the order A-like < B_I-like < B_{II}-like < A_{II}-like (see Table 2). The $O_{2'}{-}H_{O'2}{\cdots}O_2$ hydrogen bond is absent from both S conformations (Figure 4b). The small energy gap between the A-like and B_I-like conformations, does not agree with the prevalence of the N-type in double-stranded RNA.

To get a model where the A-like conformation is favored, we have to consider the presence of an explicit water molecule. In the RNA crystallographic structure,[11] O_{WT} is close enough to O_2 and $O_{2'}$ to form two hydrogen bonds. As in our model 1, $H_{O'2}$ is set away from $O_{3'}$, we considered that H_{2WT} was donated to O_2 and $H_{O'2}$ was donated to O_{WT}. After minimization at the B3LYP/6-31G(d) level of theory, four energy minima corresponding to A, A_{II}, B_I, and B_{II} analogues are obtained. The interactions of the water molecule with the O_2 of the uracil and with the 2′-OH group are kept. In the A-like, A_{II}-like, B_I-like, and B_{II}-like conformations, the O_{WT}-to-$H_{O'2}$ distance is equal to 1.78, 1.78, 1.78, and 1.79 Å, respectively, and the O_2-to-H_{2WT} distance is equal to 1.83, 1.84, 1.88, and 1.90 Å, respectively. Finally, H_{1WT} is not involved in any hydrogen bond (Figure 4c). The four minimized conformations appear in the order A-like < A_{II}-like < B_I-like < B_{II}-like (see Table 2). The energy gap between the B_I-like and the A-like conformations is large enough to favor the A-like conformation over the B_I-like conformation. Also, the A_{II}-like conformation is more stable than either of the S-type conformations.

Model 2 ($H_{O'2}$ Points to $O_{3'}$). In vacuo, at the B3LYP/6-31G(d) level of theory, we obtained three minima that agree very well with A, B_I, and B_{II} analogues. For each conformation, the values of dihedral angles β, γ, δ (not shown), ϵ, and χ (Table 3) lie in their conformational ranges. The A_{II}-like conformation is not found. The three minima appear in the order A-like < B_I-like < B_{II}-like (see Table 3). The most favorable conformation is A-like, as is required. In both N and S conformations, $H_{O'2}$ interacts with $O_{3'}$ (Figure 5a). The $O_{2'}{-}H_{O'2}{\cdots}O_{3'}$ hydrogen bond is stronger in the A-like conformation, in agreement with the literature.[7] However, the absolute value of the estimated energy gap between the A-like and the B_I-like conformations for a uracil at the B3LYP/6-31G(d) level of theory is much less than the corresponding value (2.3 kcal/mol) found for a ribose attached to an imidazole group at the MP2/6-31G(d) level.[7]

In implicit solvent, at the B3LYP/CPCM/6-31G(d) level of theory, we obtained three minima that agree with A, B_I, and B_{II} analogues (Table 3). For each conformation, the values of dihedral angles β, γ, δ (not shown), ϵ, and χ (Table 3) lie in their conformational ranges. As in vacuo, the minimization of a starting conformation similar to A_{II}-like gave the A-like conformation. The three minima appear in the order B_I-like <A-like < B_{II}-like (see Table 3). Thus, B_I-like is more stable than A-like, and therefore, these calculations do not agree with experimental data concerning double-stranded RNAs.

An explicit water molecule was then considered in model 2. Its oxygen is set as described by the X-ray data.[11] When $H_{O'2}$ points to $O_{3'}$, the protons H_{1WT} and H_{2WT} can be donated to $O_{2'}$ and O_2, respectively. Three energy minima corresponding to the A, B_I, and B_{II} analogues are obtained. As in vacuo and in implicit solvent, the A_{II}-like conformation is not found. The three minimized conformations appear in the order: A-like < B_{II}-like < B_I-like (Table 3) and the A-like conformation is by far the most favorable conformation. In the three minimized conformations, $H_{O'2}$ and the water molecule after minimization remained in similar orientations to those initially chosen (Figure 5b). In particular, after minimizations, $H_{O'2}$ still interacts with $O_{3'}$, in both the N and the S conformations. In the A-like, B_{II}-like, and B_I-like conformations, the distances separating $O_{3'}$ from $H_{O'2}$ are 2.05, 2.06, and 2.22 Å, respectively. The position of the water molecule is stabilized by hydrogen bonds between H_{1WT} and $O_{2'}$ and between H_{2WT} and O_2. In the A-like, B_{II}-like, and B_I-like conformations, the H_{1WT}-to-$O_{2'}$ distance is 2.10, 2.02, and 2.03 Å; and the H_{2WT}-to-O_2 distance is 2.06, 2.14, and 2.14 Å, respectively. In the A-like conformation, there is a

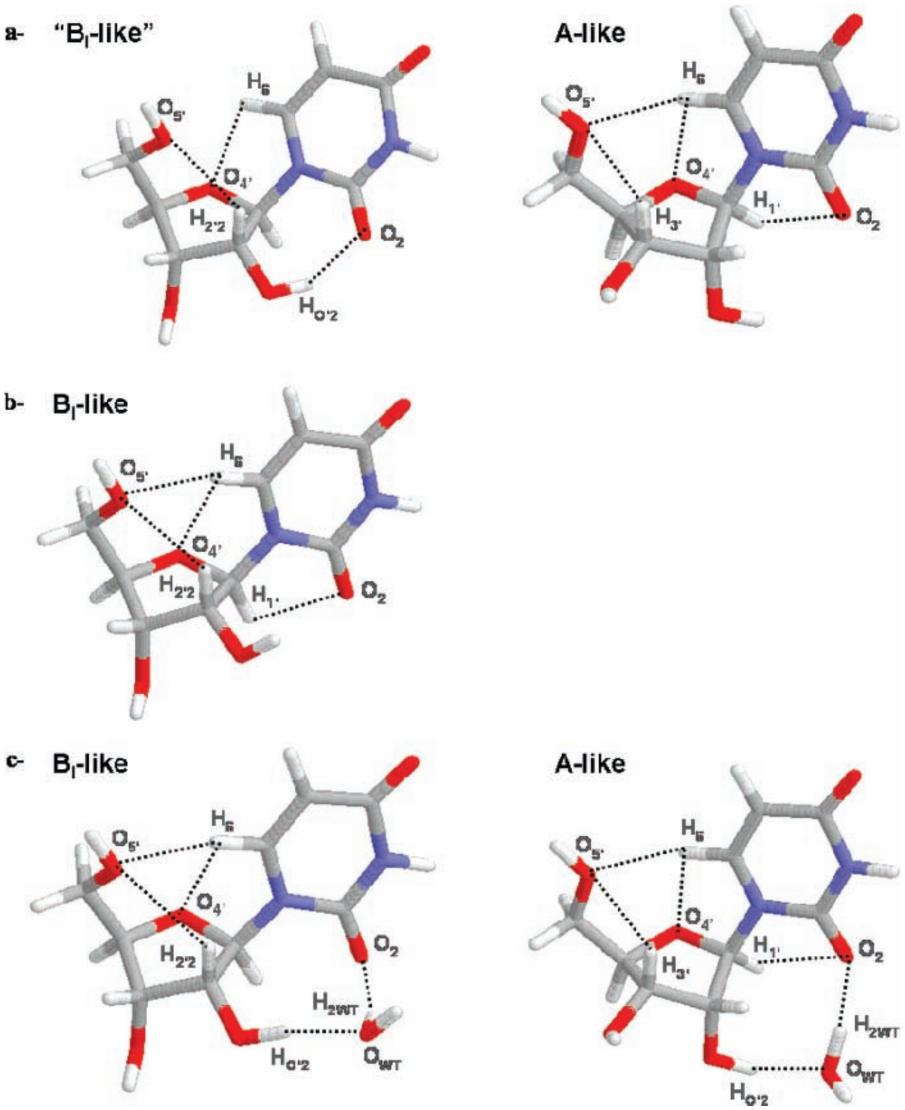

Figure 4. "B$_I$-like" and A-like conformations of OH-RIB-U (model 1: H$_{O'2}$ away from O$_{3'}$) obtained by geometry optimization at the B3LYP/6-31G(d) level of theory (a). B$_I$-like conformation of OH-RIB-U (model 1) obtained by geometry optimization from the B3LYP/CPCM/6-31G(d) method of calculation (b). B$_I$-like and A-like conformations of OH-RIB-U (model 1) obtained by geometry optimization from the B3LYP/6-31G-(d)+WT method of calculation (c). Hydrogen bonds are represented with dashed lines.

TABLE 3: Conformational Angles (Degrees) and Energy Values (Kilocalories per Mole) of OH-RIB-U in Model 2 (H$_{O'2}$ Points to O$_{3'}$)[a]

method of calculation	P	τ	ϵ	χ	ΔE_2	analogous form
B3LYP/6-31G(d)	13.78	36.8	−157.50	−158.53	−0.48	A
	164.26	36.2	−81.56	−124.53	0.15	B$_{II}$
	158.44	33.7	−155.00[b]	−127.36	0.00	B$_I$
B3LYP/CPCM/6-31G(d)	12.09	35.5	−157.50	−157.22	0.09	A
	172.32	36.8	−81.72	−125.46	0.22	B$_{II}$
	171.43	32.8	−166.81	−125.28	0.00	B$_I$
B3LYP/6-31G(d) + WT	16.67	35.4	−155.84	−163.47	−2.34	A
	165.10	35.1	−85.65	−126.98	−0.15	B$_{II}$
	159.68	30.8	−155.72	−129.59	0.00	B$_I$

[a] ΔE_2 is reported relative to the energy of the model 2 B$_I$-like conformation. P, τ, ϵ, and χ are defined in the methods section. [b] Dihedral angle ϵ constrained during the minimization.

supplementary hydrogen bond between the O$_{WT}$ of the water molecule and the H$_{1'}$ of the sugar (Figure 5b).

For an easy comparison, the energies of all conformations are reported relative to the energy of the conformation B$_I$-like of model 1 (Table 4). In vacuo and in the presence of a continuum, the most favorable conformation has an S puckering. The N-type form is clearly favored over S-type forms when a water molecule is set between O$_{2'}$ and O$_2$. This strongly indicates that water plays an important role. Finally, we note that the orientation of H$_{O'2}$ in the best conformation found here (A-like, model 1) agrees with NMR studies.[13]

OCH3-RIB-U. In all X-ray and NMR studies, on double-stranded nucleic acids containing 2′-O-methyl residues, the modified nucleoside has the N puckering.[18−22] Moreover, the orientation of the methyl group is known. Molecular dynamic simulations[64] and crystallographic[19,22] and NMR[20] data show

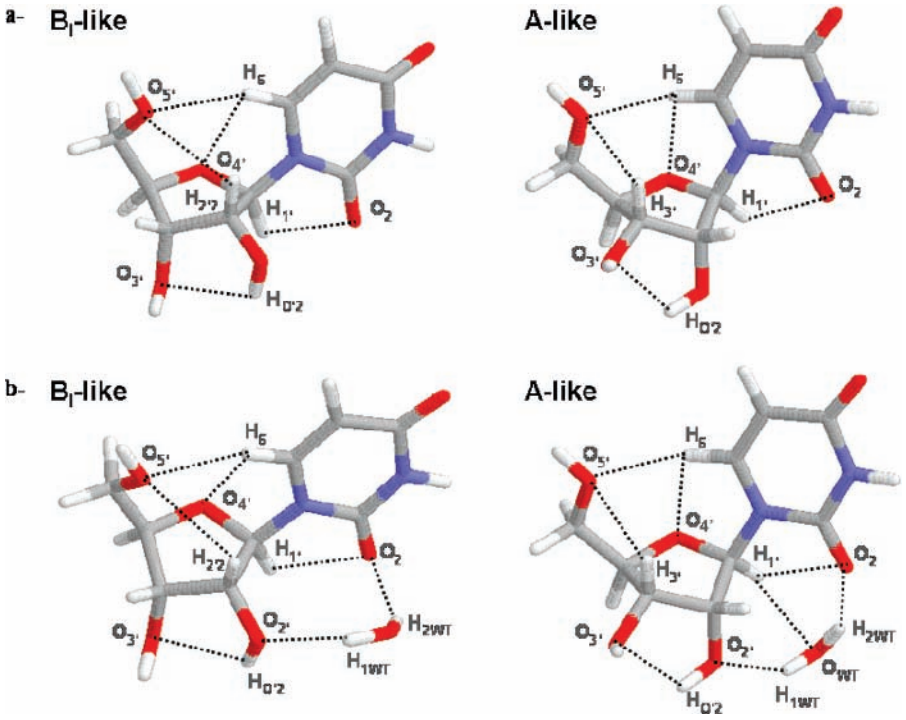

Figure 5. B_I-like and A-like conformations of OH-RIB-U (model 2: $H_{O'2}$ points to $O_{3'}$) obtained by geometry optimization at the B3LYP/6-31G-(d) level of theory (a). B_I-like and A-like conformations of OH-RIB-U (model 2) obtained by geometry optimization from the B3LYP/6-31G-(d)+WT method of calculation (b). Hydrogen bonds are represented with dashed lines.

TABLE 4: OH-RIB-U: Comparison of the Models (2nd Column)[a]

method of calculation	models	analogous form	ΔE_1
B3LYP/6-31G(d)	1	"B_I"	0.00
	2	A	0.17
	2	B_I	0.65
	2	B_{II}	0.80
	1	A	2.67
	1	"B_{II}"	3.17
	1	A_{II}	3.60
B3LYP/CPCM/6-31G(d)	2	B_I	−1.88
	2	A	−1.79
	2	B_{II}	−1.66
	1	A	−0.02
	1	B_I	0.00
	1	B_{II}	0.38
	1	A_{II}	0.42
B3LYP/6-31G(d) + WT	1	A	−2.06
	1	A_{II}	−1.33
	1	B_I	0.00
	2	A	0.51
	2	B_{II}	2.70
	2	B_I	2.85
	1	B_{II}	3.58

[a] For each method (1st column), the conformations are sorted by increasing energies ΔE_1 (kilocalories per mole, 4th column) reported to the same energy reference (0 is the energy of the B_I-like conformation of model 1).

that the 2′-OCH3 group is preferentially oriented away from $O_{3'}$ toward the minor groove in 2′-OCH3 $(CpG)_n$ duplexes. Moreover, molecular dynamic simulation of the DNA/RNA hybrid sequence d(CCAACGTTGG).r(CCAACGUUGG) with modifications at the $C_{2'}$ positions of the DNA strand by 2′-OCH3 shows that the 2′-OCH3 is also oriented away from the $O_{3'}$ atom.[65] The same orientation was also found in the crystal structure of a 2′-OCH3 adenosine incorporated into a DNA duplex.[18] Therefore, experimental data show that the methyl points to the minor groove. The methyl group at 2′ cannot fully point toward $O_{3'}$ because of steric hindrances with the phosphate group on the 3′ side,[66] namely, O_{2P}, $O_{5'}$ and to a lesser extent $H_{5'1}$, for $-43° < \lambda < 140°$.

Finally, the hydration of 2′-O-methyl duplexes is documented. 2′-OCH3 $(CpG)_3$ crystals show that no water molecule donates a proton to $O_{2'}$.[19,22] Water molecules donate a proton to cytosine O_2, and their oxygen attracts the hydrogen atoms of the methyl group.

We have determined the best conformations of OCH3-RIB-U in various hydration conditions. As for OH-RIB-U, we prevented the terminal H_{3T} hydrogen from being involved in a hydrogen bond with the adjacent 2′ group. Only the orientation of the methyl group toward the minor groove is presented here, because of the steric hindrances with the phosphate group in 3′ in real-life nucleic acids

The results are shown in Table 5. Whatever the condition of hydration, four minima are obtained: two with N puckering and two others with S puckering. The values of dihedral angles β, γ, δ (not shown), ϵ, and χ (Table 5) lie in their modal ranges, so the minimized conformations agree very well with analogues of A, A_{II}, B_I, and B_{II}.

In vacuo, the four minimized conformations appear in the order A-like < B_I-like < A_{II}-like < B_{II}-like (Table 5). The A-like−B_I-like gap is only 0.13 kcal/mol. The final optimized conformations are shown in Figure 6a. The hydrogen bonds stabilizing the B_I-like and the A-like conformations of OCH3-RIB-U are the four canonical hydrogen bonds that stabilize the S and N conformation, respectively (Figure 6a).

In implicit solvent, the minimized conformations appear in the order B_I-like < A-like < A_{II}-like < B_{II}-like (Table 5). The B_I-like conformation is only slightly more stable than the A-like conformation. Moreover, the energy differences with the other conformations are also relatively small. Although the B_{II}-like conformation is the most unfavorable conformation, it is much less unfavorable than in vacuo. Therefore, OCH3-RIB-U is very flexible in implicit solvent. The hydrogen bonds stabilizing the S and N conformations of OCH3-RIB-U in implicit solvent are

TABLE 5: Conformational Angles (Degrees) and Relative Energy Values (Kilocalories per Mole) of OCH3-RIB-U (Methyl Group Is Away from $O_{3'}$)[a]

method of calculation	P	τ	ϵ	χ	ΔE	analogous form
B3LYP/6-31G(d)	14.69	40.2	−92.23	−158.26	0.43	A_{II}
	13.66	38.1	−155.00[b]	−158.77	−0.13	A
	170.62	35.9	−71.55	−126.10	2.83	B_{II}
	166.64	34.3	−155.00[b]	−127.95	0.00	B_I
B3LYP/CPCM/6-31G(d)	11.80	38.1	−92.33	−156.32	0.44	A_{II}
	11.38	37.0	−155.00[b]	−155.91	0.04	A
	177.34	36.6	−68.31	−125.93	0.63	B_{II}
	175.59	34.9	−155.00[b]	−125.34	0.00	B_I
B3LYP/6-31G(d) + WT	12.76	41.0	−93.50	−157.65	0.09	A_{II}
	12.15	38.9	−155.00[b]	−157.38	−0.47	A
	170.51	37.0	−72.53	−120.26	2.98	B_{II}
	166.99	35.4	−155.00[b]	−121.25	0.00	B_I

[a] ΔE is reported relative to the energy of the B_I-like conformation. P, τ, ϵ and χ are defined in the methods section. [b] Dihedral angle ϵ constrained during the minimization.

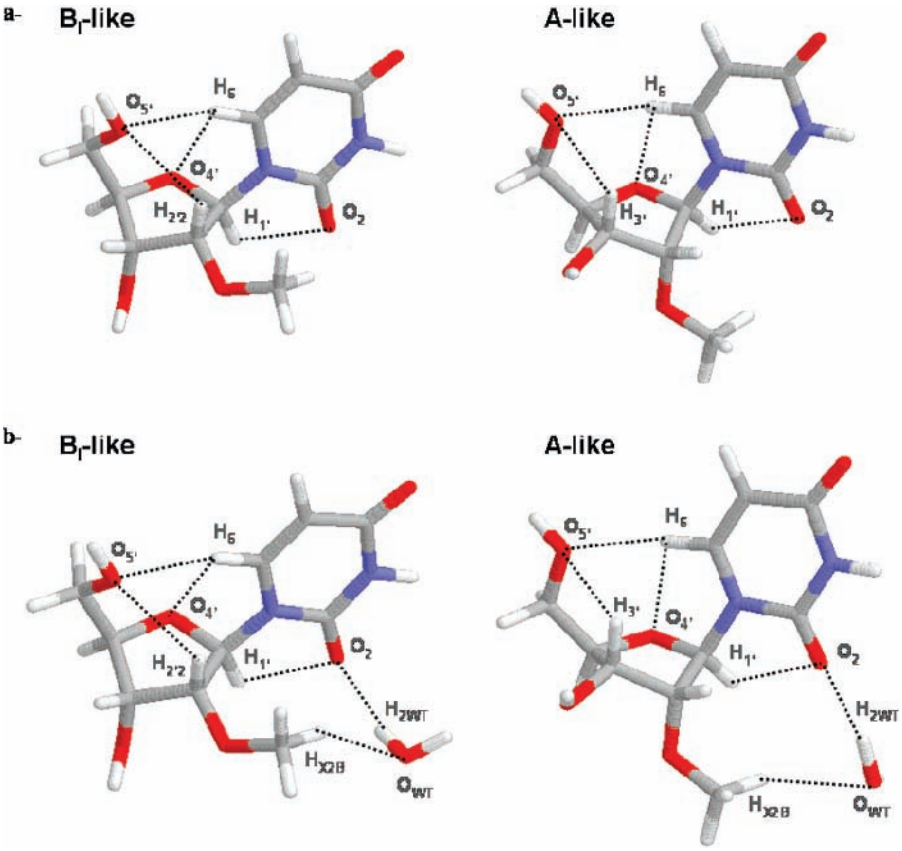

Figure 6. B_I-like and A-like conformations of OCH3-RIB-U obtained by geometry optimization at the B3LYP/6-31G(d) level of theory (a). B_I-like and A-like conformations of OCH3-RIB-U (model 1) obtained by geometry optimization from the B3LYP/6-31G(d)+WT method of calculation (b). Hydrogen bonds are represented with dashed lines.

similar to those stabilizing these conformations in vacuo, as expected by the very minor effect of the solvation model on the geometry.

In the presence of an explicit water molecule donating a proton to uracil O_2 and accepting a proton from the 2′-methyl group, the minimized conformations appear in the order A-like < B_I-like < A_{II}-like < B_{II}-like (Table 5) which is identical to the ranking in vacuo without the explicit water molecule. In the presence of the water molecule, the A-like conformation is more stable than the B_I-like conformation by 0.47 kcal/mol. This energy gap between the A-like and the B_I-like conformations is much smaller for OCH3-RIB-U than for OH-RIB-U (Table 2). Therefore, OCH3-RIB-U seems to have a more flexible sugar puckering than OH-RIB-U. In all conformations, the O_{WT} atom of the water molecule is close to the methyl group. In the A-like, B_I-like, A_{II}-like, and B_{II}-like conformations, the O_{WT} to H_{X2B} distance is 2.48, 2.44, 2.46, and 2.46 Å, respectively. Moreover, H_{2WT} points to the uracil O_2, with the O_2-to-H_{2WT} distance being 1.94 Å in all four conformations (Figure 6b). To summarize, in vacuo, the A-like conformation is the most favorable conformation, but the A-like-B_I-like gap is small. In implicit water, the B_I-like is the best, by a narrow edge. An explicit water molecule forming a bridge between the 2′-OCH3 and the uracil O_2 has a small effect on the A-like−B_I-like gap.

East Energy Barriers. We have calculated the east energy barriers, Be (see Methods), in H−U, OH-RIB-U (models 1 and 2), and OCH3-RIB-U (see Table 6). For OH-RIB-U and OCH3-RIB-U, in the $O_{4'}$ endo conformations, the ϵ dihedral angle was constrained at −155.0° to avoid the formation of the $O_{3'}-H_{3T'}\cdot$

TABLE 6: Estimates of the East Barriers (Be) for the Compounds Studied[a]

compound	model	method of calculation	Be	τ
H−U		B3LYP/6-31G(d)	2.34	17.7
		B3LYP/CPCM/6-31G(d)	2.82	12.0
		B3LYP/6-31G(d) + WT	1.68	15.4
OH−RIB−U	1	B3LYP/6-31G(d)	2.76	29.4
		B3LYP/CPCM/6-31G(d)	3.68	36.5
		B3LYP/6-31G(d) + WT	3.28	14.7
OH−RIB−U	2	B3LYP/6-31G(d)	2.46	22.9
		B3LYP/CPCM/6-31G(d)	2.96	20.0
		B3LYP/6-31G(d) + WT	2.44	24.0
OCH3-RIB−U		B3LYP/6-31G(d)	2.58	19.5
		B3LYP/CPCM/6-31G(d)	2.71	15.3
		B3LYP/6-31G(d) + WT	3.34	17.4

[a] Energy Be (kilocalories per mole) and the puckering amplitude τ are calculated for the $O_{4'}$ endo ($\tau_2 = 0°$) conformations.

TABLE 7: Single Point Energy of the Same Conformation (OH-RIB-U, Model 1) at Different Theory Levels[a]

theory level	energy (Hartrees)
HF/6-31G(d)	−905.875446284
MP2/6-31G(d)	−908.408244305
B3LYP/6-31G(d)	−911.015336657
B3LYP/6-311++G(2df,2pd) SCF=Tight	−911.365947762
B3LYP/6-311++G(3df,3pd) SCF=Tight	−911.375474635
B3LYP/6-311++G(2df,2pd) SCF=Tight	−911.376577669

[a] First, OH-RIB-U is optimized using B3LYP/6-31G(d). Then, its single point energy is calculated (column 2) at various theory levels (column 1).

$\cdot\cdot O_{2'}$ hydrogen bond. The 2′-OH was oriented as in the models 1 or 2 by constraining λ in a preliminary minimization. The resulting conformation was optimized during a second minimization with the dihedral λ unconstrained.

The Be values differ according to the hydration conditions (Table 6).

H−U. The value of Be determined at the B3LYP/6-31G(d) level of theory (Table 6) is approximately half that calculated at the MP2/6-31G(d) level of theory.[51] In contrast, the value of Be at the B3LY/6-31G(d) level agrees with those estimated for other deoxynucleosides at the same level of theory.[50,67] Therefore, the Be are significantly sensitive to the level of theory used.

The $O_{4'}$ endo conformation of H−U is associated with a significant flattening of the furanose ring: the furanose amplitude τ at the east barrier is significantly lower than in the N and S energy minima as shown for standard deoxyribonucleosides.[51]

OH-RIB-U. Be values are higher in model 1 than in model 2 (Table 6).

Model 1. In vacuo, in implicit solvent and in the presence of an explicit water molecule, the Be for OH-RIB-U are higher than those for H−U by 0.42 kcal/mol, 0.86 kcal/mol, and 1.60 kcal/mol, respectively. Our last estimate, in the presence of the explicit water molecule (1.60 kcal/mol) is the closest to Olson's prediction[42] (2.0 kcal/mol). Only, in the presence of the explicit water molecule, the amplitude τ at the east barrier is significantly lower than that in the N and S energy minima, as observed in H−U.

Model 2. The Be determined at the B3LYP/6-31G(d) level of theory (Table 6) are half that calculated at the MP2/6-31G(d) level for a ribose bound to an imidazole group.[7] This difference may be a consequence of the replacement of the base by an imidazole group or of the level of theory used, as shown for H−U. In vacuo, in implicit solvent and in the presence of the explicit water molecule, the Be for OH-RIB-U are higher than the Be for H−U by 0.12, 0.14, and 0.56 kcal/mol, respectively. These values are smaller than the difference between the Be in ribose and that in deoxyribose predicted by Olson.[42] The value determined in the presence of the explicit water molecule (0.56 kcal/mol) is similar to the difference between the Be in a ribose and a deoxyribose bound to an imidazole group.[7] The furanose amplitude τ at the east barriers is lower than that in the N and S energy minima. However, this flattening of the furanose ring in the O4′ endo conformations is less significant than in H−U east conformations.

OCH3-RIB-U. In vacuo, in both the absence and the presence of the explicit water molecule, the Be (Table 6) are higher than those for H−U by 0.24 kcal/mol and 1.66 kcal/mol, respectively.

The barriers are related to the pucker interconversion time rate. If only the hydrated models are retained, OCH3-RIB-U and OH-RIB-U in model 1 would dynamically toggle their puckering significantly slower than H−U.

Data Accuracy. DFT methods are very popular within the biochemical community[68,69] because high quality computations on large systems can be performed using reasonable computer time. In contrast to the simple Hartree−Fock (HF) method, DFT treats the electron correlation correctly. In principle, DFT methods give a good estimate of Coulombic interactions but fail when charge transfers or dispersion forces contribute significantly. The DFT approach suffers severe limitations in the treatment of interbase interaction in nucleic acids[69] or in the prediction of properties of molecules like CrCO.[70] Moreover, the MP2 method ameliorates significantly the HF calculations because it treats the electron correlation in a better way. Recently, it has been used in a sophisticated way to evaluate the anomeric effect.[71] As the HF, MP2, and B3LYP do not evaluate the energy contributions in the same way, it is interesting to compare their results on the same conformations.

The energy of the OH-RIB-U model 1 conformation optimized at the B3LYP/6-31G(d) level was estimated using various techniques (Table 7). HF and MP2 energies are much higher than the B3LYP energies that seem to be weakly sensitive on the quality of the basis set (Table 7). The differences between all of these estimates are very large (several Hartrees) when compared with the energy gaps presented in Tables 1−6 (most values being less than some kcal/mol).

The energies of various conformations are reported relative to the energy of the corresponding B_I-like conformation using four different methods (see Table 8). The conformations are sorted according to increasing B3LYP/6-31G(d) energy differences. In most cases, the energy differences are found in the same order. This means that MP2 method does not bring a significant improvement as is the case for deoxynucleosides.[50] The main inversion concerns the A-like conformation of OH-RIB-U in vacuo. Interestingly, the most favorable conformation of model 2 ribose derivatives have been described in the N puckering in the literature[7,52] using the MP2 method. However, this conformation does not agree with the orientation of $H_{O'2}$ as determined by NMR.[13] Moreover the energy gap is too small to confer rigidity to the ribose in duplexes. That is why the model in vacuo should be rejected. Finally, when the water molecule is present, all methods agree and agree with experiment. The right orientation of $H_{O'2}$ is found. The energy gap is sufficiently large to ensure the prevalence of the N puckering.

All methods agree in the case of OCH3-RIB-U. It may easily change its pucker, and the water molecule has no sensitive effect.

TABLE 8: Single Point Energy Calculations on Several Conformations[a]

OH−RIB−U without a water molecule

analogous form	model	HF/6-31G(d)	MP2/6-31G(d)	B3LYP/6-31G(d)	B3LYP/6-311++G(3df,2pd)
B_I	1	0.00	0.00	0.00	0.00
A	2	0.34	−0.62	0.17	0.21
B_I	2	0.31	0.50	0.65	0.02
B_{II}	2	0.42	0.41	0.80	0.30
A	1	1.49	2.23	2.67	1.58
A_{II}	1	2.51	2.90	3.60	2.41

OH−RIB−U with a water molecule

analogous form	model	HF/6-31G(d)	MP2/6-31G(d)	B3LYP/6-31G(d)	B3LYP/6-311++G(3df,2pd)
A	1	−2.26	−2.42	−2.06	−2.04
A_{II}	1	−1.39	−1.89	−1.33	−1.28
B_I	1	0.00	0.00	0.00	0.00
A	2	−0.14	−0.56	0.51	1.51
B_{II}	2	0.71	1.41	2.70	1.82
B_I	2	1.13	1.99	2.85	1.93

OCH3-RIB−U without a water molecule

analogous form	HF/6-31G(d)	MP2/6-31G(d)	B3LYP/6-31G(d)	B3LYP/6-311++G(2df,2pd)
A	−0.58	−0.11	−0.13	−0.38
B_I	0.00	0.00	0.00	0.00

OCH3-RIB−U with a water molecule

analogous form	HF/6-31G(d)	MP2/6-31G(d)	B3LYP/6-31G(d)	B3LYP/6-311++G(2df,2pd)
A	−0.89	−0.42	−0.47	−0.40
B_I	0.00	0.00	0.00	0.00

[a] Some conformations optimized at the B3LYP/6-31G(d) were recalculated using different theory levels. The energies (kilocalories per mole) are reported to the B_I-like (model 1) of each system.

Conclusion

How a stable double stranded polynucleotide can have a smooth regular general structure whereas it is made of diverse structural units? As the helical structure does not deeply depend either on the length of the polynucleotide or on its sequence, each residue must share with the others a conformation of relative minimum energy. Of course, the building of the polymer requires some energy to distort each monomer from its solution structure to the conformation it has in the polynucleotide. But, if there are no collective or long-range effects, the general assembly is stable, as each residue is in a conformational energetic minimum. Therefore, it should be possible to predict the conformation of a nucleotide inserted in a duplex by generating optimized structures compatible with the helical structure of the polynucleotide. When several conformations are found, the flexibility is directly related to the energy gaps. Finally, the height of the energy barrier between the conformations should give an estimate of the rate of transition between the various conformations.

In this paper, three nucleosides have been studied: H−U, OCH3-RIB-U, and OH-RIB-U. The computations in vacuo give the expected result for the most favorable conformation: H−U is S, and OCH3-RIB-U is N. In vacuo, OH-RIB-U is found in the N orientation but only in model 2 when the hydroxyl at $O_{2'}$ points toward $O_{3'}$, while NMR data report it in the opposite orientation.[13] Moreover, the energy gap A-like−B_I-like in OH-RIB-U is similar to the energy gap B_I-like−A-like in H−U. This means that the population of OH-RIB-U in the S puckering should be as significant as the population of H−U in the N puckering. Because the model in vacuo fails, we studied the effect of hydration. We first embedded the nucleosides H−U, OCH3-RIB-U, or OH-RIB-U, in a continuum to mimick the dielectric properties of bulk water. The most stable conformation of OH-RIB-U is still S. Here, the predictions failed either because the water molecules that are close to the nucleic acids in vitro are not sufficiently mobile to give a dielectric constant close to that of bulk water, or because the nucleoside is only partially in contact with water, when it belongs to a duplex.

We thus, investigated the effect of a water molecule. We could have studied exhaustively all the hydration sites. However, in our model, the binding of a water molecule to $O_{2'}$ on the $O_{3'}$ side cannot be studied reliably because of the proximity of H_{3T} atom in our model. We introduced a water molecule, donating a proton to O_2 and interacting with the 2′ group, as experimentally described.[11,19,22] For H−U or OCH3-RIB-U, the effect of a single water molecule is found to be qualitatively small.

In contrast, for OH-RIB-U, the role of the water molecule is crucial: the most stable conformation is N. The energy gap between the A-like and the B_I-like forms is very large which ensures the absence of S puckering in RNA double helices. For OCH3-RIB-U, the gap A-like−B_I-like slightly increases. The interaction between the lone pairs of $O_{2'}$ and $O_{3'}$ might be responsible for the effect of the presence of a water molecule. In the model 1 of OH-RIB-U and in OCH3-RIB-U, the lone-pairs interact unfavorably. The presence of a water molecule decreases the density of the $O_{2'}$ lone pair in the 2′-OH compound efficiently. In the model 2 of OH-RIB-U, the lone pairs of $O_{2'}$ and $O_{3'}$ do not interact. In the presence of the methyl group, the water molecule cannot polarize the $O_{2'}$−$H_{O'2}$ bond efficiently.

According to our calculations, the sugar puckering of OCH3-RIB-U should be more flexible than that of OH-RIB-U. Experimental[20] and theoretical[64] studies show that the pucker of r(CG)n fluctuates slightly more than that of 2′-O-Me(CG)n. The proximity of other methyl groups and interstrand interactions may organize hydration in a way that cannot be determined from the study of just one nucleoside.

It is interesting that a unique water molecule has such a drastic effect on the puckering of OH-RIB-U. Positions of the oxygen atom of water molecules that have been found close to the nucleic acid bases can be found on the Internet.[72] As there is an accumulation at only one site explored here, the position is certainly important. However, water molecules at other positions might play a role to be determined in future work.

Acknowledgment. S.B. is grateful for a MNRT fellowship. Access to the ENS-Cachan computing facilities is acknowledged.

Supporting Information Available: Hydrogen bond lengths (proton−acceptor distance in Å) for the conformations optimized at the B3LYP/6-31G(d) level and shown in the figures of the paper. This material is available free of charge via the Internet at http://pubs.acs.org.

References and Notes

(1) Saenger, W. *Principles of Nucleic Acid Structure*; Springer-Verlag: New York, 1984.

(2) Shindo, H.; Fujiwara, T.; Akutsu, H.; Matsumoto, U.; Kyogoku, Y. *Biochemistry* **1985**, *24*, 887.

(3) Cheatham, T. E.; Kollman, P. A. *J. Am. Chem. Soc.* **1997**, *119*, 4805.

(4) Auffinger, P.; Westhof, E. *J. Mol. Biol.* **2000**, *300*, 1113.

(5) MacKerell, A. D.; Banavali, N. *J. Comput. Chem.* **2000**, *21*, 105.

(6) Berman, H. M.; Olson, W. K.; Beveridge, D. L.; Westbrook, J.; Gelbin, A.; Demeny, T.; Hsieh, S. H.; Srinivasan, A. R.; Schneider, B. *Biophys. J.* **1992**, *63*, 751.

(7) Foloppe, N.; MacKerell, A. D. *J. Phys. Chem. B* **1998**, *102*, 6669.

(8) Fersht, A. R. *Enzyme Structure and Mechanism*; W. H. Freeman & Co: San Francisco, 2005.

(9) Rousse, B.; Puri, N.; Viswanadham, G.; Agback, P.; Glemarec, C.; Sandstrom, A.; Sund, C.; Chattopadhyaya, J. *Tetrahedron* **1994**, *50*, 1777.

(10) Cech, T. R. *Annu. Rev. Biochem.* **1990**, *59*, 543.

(11) Egli, M.; Portmann, S.; Usman, N. *Biochemistry* **1996**, *35*, 8489.

(12) Acharya, P.; Chattopadhyaya, J. *J. Org. Chem.* **2002**, *67*, 1852.

(13) Gyi, J. I.; Lane, A. N.; Conn, G. L.; Brown, T. *Nucleic Acids Res.* **1998**, *26*, 3104.

(14) Auffinger, P.; Westhof, E. *J. Mol. Biol.* **1997**, *274*, 54.

(15) Freier, S. M.; Altmann, K. H. *Nucleic Acids Res.* **1997**, *25*, 4429.

(16) Kierzek, E.; Ciesielska, A.; Pasternak, K.; Mathews, D. H.; Turner, D. H.; Kierzek, R. *Nucleic Acids Res.* **2005**, *33*, 5082.

(17) Agapkina, J.; Smolov, M.; Barbe, S.; Zubin, E.; Zatsepin, T.; Deprez, E.; Le Bret, M.; Mouscadet, J. F.; Gottikh, M. *J. Biol. Chem.* **2006**.

(18) Lubini, P.; Zurcher, W.; Egli, M. *Chem. Biol.* **1994**, *1*, 39.

(19) Adamiak, D. A.; Rypniewski, W. R.; Milecki, J.; Adamiak, R. W. *Nucleic Acids Res.* **2001**, *29*, 4144.

(20) Popenda, M.; Biala, E.; Milecki, J.; Adamiak, R. W. *Nucleic Acids Res.* **1997**, *25*, 4589.

(21) Nishizaki, T.; Iwai, S.; Ohtsuka, E.; Nakamura, H. *Biochemistry* **1997**, *36*, 2577.

(22) Adamiak, D. A.; Milecki, J.; Popenda, M.; Adamiak, R. W.; Dauter, Z.; Rypniewski, W. R. *Nucleic Acids Res.* **1997**, *25*, 4599.

(23) Buckin, V. A. *Mol. Biol.* **1987**, *21*, 512.

(24) Saenger, W. *Annu. Rev. Biophys. Biophys. Chem.* **1987**, *16*, 93.

(25) Westhof, E. *Annu. Rev. Biophys. Biophys. Chem.* **1988**, *17*, 125.

(26) Misra, V. K.; Sharp, K. A.; Friedman, R. A.; Honig, B. *J. Mol. Biol.* **1994**, *238*, 245.

(27) Chalikian, T. V.; Plum, G. E.; Sarvazyan, A. P.; Breslauer, K. J. *Biochemistry* **1994**, *33*, 8629.

(28) Shakked, Z.; Guzikevich-Guerstein, G.; Frolow, F.; Rabinovich, D.; Joachimiak, A.; Sigler, P. B. *Nature* **1994**, *368*, 469.

(29) Otwinowski, Z.; Schevitz, R. W.; Zhang, R. G.; Lawson, C. L.; Joachimiak, A.; Marmorstein, R. Q.; Luisi, B. F.; Sigler, P. B. *Nature* **1988**, *335*, 321.

(30) Olmsted, M. C. *J. Biomol. Struct. Dyn.* **1996**, *13*, 885.

(31) Robinson, C. R.; Sligar, S. G. *J. Mol. Biol.* **1993**, *234*, 302.

(32) Qian, Y. Q.; Otting, G.; Wuthrich, K. *J. Am. Chem. Soc.* **1993**, *115*, 1189.

(33) Falk, M.; Lord, R.; Hartman, K. *J. Am. Chem. Soc.* **1962**, *84*, 3843.

(34) Dickerson, R. E.; Drew, H. R.; Conner, B. N.; Wing, R. M.; Fratini, A. V.; Kopka, M. L. *Science* **1982**, *216*, 475.

(35) Ouali, M.; Gousset, H.; Geinguenaud, F.; Liquier, J.; Gabarro-Arpa, J.; Le Bret, M.; Taillandier, E. *Nucleic Acids Res.* **1997**, *25*, 4816.

(36) Tolstorukov, M. Y.; Jernigan, R. L.; Zhurkin, V. B. *J. Mol. Biol.* **2004**, *337*, 65.

(37) Wiberg, K. B.; Murcko, M. A.; Laidig, K. E.; Macdougall, P. J. *J. Phys. Chem.* **1990**, *94*, 6956.

(38) Murcko, M. A.; Dipaola, R. A. *J. Am. Chem. Soc.* **1992**, *114*, 10010.

(39) Phillips, L.; Wray, V. *J. Chem. Soc., Chem. Commun.* **1973**, 90.

(40) Thibaudeau, C.; Plavec, J.; Chattopadhyaya, J. *J. Am. Chem. Soc.* **1994**, *116*, 8033.

(41) Plavec, J.; Tong, W. M.; Chattopadhyaya, J. *J. Am. Chem. Soc.* **1993**, *115*, 9734.

(42) Olson, W. K. *J. Am. Chem. Soc.* **1982**, *104*, 278.

(43) Plavec, J.; Thibaudeau, C.; Chattopadhyaya, J. *Pure Appl. Chem.* **1996**, *68*, 2137.

(44) Oleary, D. J.; Kishi, Y. *J. Org. Chem.* **1994**, *59*, 6629.

(45) Kneisler, J. R.; Allinger, N. L. *J. Comput. Chem.* **1996**, *17*, 757.

(46) Jaffe, R. L.; Smith, G. D.; Yoon, D. Y. *J. Phys. Chem.* **1993**, *97*, 12745.

(47) Guschlbauer, W.; Jankowski, K. *Nucleic Acids Res.* **1980**, *8*, 1421.

(48) Uesugi, S.; Miki, H.; Ikehara, M.; Iwahashi, H.; Kyogoku, Y. *Tetrahedron Lett.* **1979**, *42*, 4073.

(49) Hocquet, A.; Leulliot, N.; Ghomi, M. *J. Phys. Chem. B* **2000**, *104*, 4560.

(50) Foloppe, N.; Nilsson, L.; MacKerell, A. D., Jr. *Biopolymers* **2001**, *61*, 61.

(51) Foloppe, N.; MacKerell, A. D. Jr. *Biophys. J.* **1999**, *76*, 3206.

(52) Brameld, K. A.; Goddard, W. A. *J. Am. Chem. Soc.* **1999**, *121*, 985.

(53) Frisch, M. J.; Trucks, G. W.; Schlegel, H. B.; Scuseria, G. E.; Robb, M. A.; Cheeseman, J. R.; Montgomery, J. J. A.; Vreven, T.; Kudin, K. N.; Burant, J. C.; Millam, J. M.; Iyengar, S. S.; Tomasi, J.; Barone, V.; Mennucci, B.; Cossi, M.; Scalmani, G.; Rega, N.; Petersson, G. A.; Nakatsuji, H.; Hada, M.; Ehara, M.; Toyota, K.; Fukuda, R.; Hasegawa, J.; Ishida, M.; Nakajima, T.; Honda, Y.; Kitao, O.; Nakai, H.; Klene, M.; Li, X.; Knox, J. E.; Hratchian, H. P.; Cross, J. B.; Bakken, V.; Adamo, C.; Jaramillo, J.; Gomperts, R.; Stratmann, R. E.; Yazyev, O.; Austin, A. J.; Cammi, R.; Pomelli, C.; Ochterski, J. W.; Ayala, P. Y.; Morokuma, K.; Voth, G. A.; Salvador, P.; Dannenberg, J. J.; Zakrzewski, V. G.; Dapprich, S.; Daniels, A. D.; Strain, M. C.; Farkas, O.; Malick, D. K.; Rabuck, A. D.; Raghavachari, K.; Foresman, J. B.; Ortiz, J. V.; Cui, Q.; Baboul, A. G.; Clifford, S.; Cioslowski, J.; Stefanov, B. B.; Liu, G.; Liashenko, A.; Piskorz, P.; Komaromi, I.; Martin, R. L.; Fox, D. J.; Keith, T.; Al-Laham, M. A.; Peng, C. Y.; Nanayakkara, A.; Challacombe, M.; Gill, P. M. W.; Johnson, B.; Chen, W.; Wong, M. W.; Gonzalez, C.; Pople, J. A. *Gaussian 03*, Revision A.1; Gaussian, Inc.: Pittsburgh, PA, 2003.

(54) Barone, V.; Cossi, M. *J. Phys. Chem. A* **1998**, *102*, 1995.

(55) Barone, V.; Cossi, M.; Tomasi, J. *J. Chem. Phys.* **1997**, *107*, 3210.

(56) Schneider, B.; Patel, K.; Berman, H. M. *Biophys. J.* **1998**, *75*, 2422.

(57) Rao, S.; Westhof, E.; Sundaralingam, M. *Acta Crystallogr., Sect. A* **1981**, *37*, 421.

(58) Le Bret, M.; Gabarro-Arpa, J.; Gilbert, J. C.; Lemarechal, C. *J. Chim. Phys.* **1991**, *88*, 2489.

(59) Winger, R. H.; Liedl, K. R.; Rudisser, S.; Pichler, A.; Hallbrucker, A.; Mayer, E. *J. Phys. Chem. B* **1998**, *102*, 8934.

(60) Desiraju, G. R. *Acc. Chem. Res.* **1996**, *29*, 441.

(61) Wahl, M. C.; Sundaralingam, M. *Trends Biochem. Sci.* **1997**, *22*, 97.

(62) Leulliot, N.; Ghomi, M.; Scalmani, G.; Berthier, G. *J. Phys. Chem. A* **1999**, *103*, 8716.

(63) Lu, X. J.; Shakked, Z.; Olson, W. K. *J. Mol. Biol.* **2000**, *300*, 819.

(64) Auffinger, P.; Westhof, E. *Angew. Chem., Int. Ed.* **2001**, *40*, 4648.

(65) Venkateswarlu, D.; Lind, K. E.; Mohan, V.; Manoharan, M.; Ferguson, D. M. *Nucleic Acids Res.* **1999**, *27*, 2189.

(66) Kawai, G.; Yamamoto, Y.; Kamimura, T.; Masegi, T.; Sekine, M.; Hata, T.; Iimori, T.; Watanabe, T.; Miyazawa, T.; Yokoyama, S. *Biochemistry* **1992**, *31*, 1040.

(67) Arora, K.; Schlick, T. *Chem. Phys. Lett.* **2003**, *378*, 1.

(68) Dobes, P.; Otyepka, M.; Strnad, M.; Hobza, P. *Chemistry* **2006**, *12*, 4297.

(69) Hobza, P.; Sponer, J. *Chem. Rev.* **1999**, *99*, 3247.

(70) Kim, J.; Lee, Y. S.; Ihee, H. *Int. J. Quantum Chem.* **2007**, *107*, 458.

(71) Woodcock, H. L.; Moran, D.; Pastor, R. W.; MacKerell, A. D., Jr.; Brooks, B. R. *Biophys. J.* **2007**, *93*, 1.

(72) Auffinger, P. *SwS*, Solvation web service for nucleic acids.